OPEN ACCESS
JOURNAL OF ADVANCED DIELECTRICS
Vol. 11, No. 2 (2021) 2150010 (9 pages)

DOI: 10.1142/S2010135X21500107

Lead-free 0–3-type composites: From piezoelectric sensitivity to modified figures of merit

Ashura N. Isaeva and Vitaly Yu. Topolov*

Department of Physics, Southern Federal University
5 Zorge Street, 344090 Rostov-on-Don, Russia

*vutopolov@sfedu.ru

Received 29 January 2021; Revised 16 March 2021; Accepted 17 March 2021; Published 9 April 2021

Effective piezoelectric properties, electromechanical coupling factors (ECF) and figures of merit (FOM) are studied in lead-free 0–3-type composites based on novel ferroelectric $0.965(K_{0.48}Na_{0.52})(Nb_{0.96}Sb_{0.04})O_3$–$0.035Bi_{0.5}Na_{0.5}Zr_{0.15}Hf_{0.75}O_3$ ceramic. Systems of prolate ceramic inclusions are surrounded by a large polymer matrix that can be either monolithic (in the 0–3 composite) or porous (in the 0–3–0 composite). Non-monotonic volume-fraction dependences of the effective piezoelectric coefficients g_{3j}^*, ECF k_{3j}^*, squared FOM $d_{3j}^* g_{3j}^*$ and their modified analogs for stress-driven systems are analysed, and examples of the high longitudinal piezoelectric sensitivity ($g_{33}^* > 100$ mV·m/N) are considered. A role of microgeometrical factors, that promote the large effective parameters and anisotropy of properties in the 0–3-type composites, is highlighted. New "aspect ratio — volume fraction" diagrams are first built to describe conditions for high piezoelectric sensitivity, large modified FOM and their anisotropy in the studied composites. These advanced materials can be of value for piezoelectric sensor, energy-harvesting and related applications.

Keywords: Lead-free 0–3-type composite; piezoelectric properties; figures of merit; electromechanical coupling factors.

1. Introduction

In the last decades, piezo-active composites were developed mainly due to use of high-effective lead-containing components, e.g., ferroelectric ceramics[1] (FCs) based on Pb(Zr, Ti)O_3 or domain-engineered relaxor-ferroelectric $(1 - x)Pb(Mg_{1/3}Nb_{2/3})O_3 - xPbTiO_3$ (PMN–xPT) and $(1 - y)$-$Pb(Zn_{1/3}Nb_{2/3})O_3 - yPbTiO_3$ single crystals.[2–4] In recent years, many efforts in the field of lead-free piezoelectrics[5–7] show that novel lead-free composites[8–11] can be a good alternative due to the strong electromechanical coupling, high piezoelectric sensitivity, large piezoelectric anisotropy and figures of merit (FOMs). Among piezo-active lead-free composites to be of interest in academic and technological senses, we mention 0–3 composites.[9,12,13] The piezo-active 0–3 composite is described[4,9] as a system of piezoelectric inclusions in a large matrix that can be either piezo-passive or piezoelectric. The 0–3 FC/polymer composites are often manufactured by means of the dielectrophoresis.[9,14,15] The dielectrophoresis means a movement of dielectric inclusions in a surrounding medium in an external inhomogeneous electric field $\boldsymbol{E}$.[9,14,15] In the case of the aforementioned 0–3 composite during dielectrophoresis, small FC particles of this composite construct the so-called chain-like structures (or highly prolate inclusions)[14,15] oriented along the $\boldsymbol{E}$ direction. As is known, a degree of alignment of these chain-like structures depends on a force that acts on the FC particles inclusions being formed in the external electric field $\boldsymbol{E}$, and this force depends on an amplitude and frequency of the electric field, on the dielectric properties of the FC and surrounding polymer components, on sizes of the FC particles,[15] and so on. The system of the highly prolate FC inclusions poled along the $\boldsymbol{E}$ vector promotes an improved piezoelectric performance of the structured composite in comparison to the related non-structured 0–3 composites.[8,15]

Moreover, novel piezo-active 0–3–0 composites with porous polymer matrices[16] exhibit characteristics that are improved in comparison to the 0–3 analogs.[15] A performance of a dielectrophoretically aligned quasi 1–3 composite based on a lead-free FC is studied by Stuber *et al*.,[9] and a high level of the piezoelectric sensitivity of the quasi 1–3 composite is highlighted.

In the literature, one can find full sets of electromechanical (i.e., elastic, piezoelectric and dielectric) constants of poled lead-free FCs,[17,18] and the lead-free compositions are often selected among ferroelectric solid solutions based on alkali niobates with the perovskite-type structure. Very recently, Qiao *et al*.[18] studied a novel $0.965(K_{0.48}Na_{0.52})(Nb_{0.96}Sb_{0.04})O_3$–$0.035Bi_{0.5}Na_{0.5}Zr_{0.15}Hf_{0.75}O_3$ (KNNS–BNZH) FC. This FC material was manufactured by means of the traditional solid-state method. KNNS–BNZH FC samples with gold electrodes were poled in silicone oil at room temperature for 5 min, and a dc electric field $E = 40$ kV/cm was applied for this poling.[18] The full set of electromechanical constants of

*Corresponding author.

the poled KNNS–BNZH FC[18] suggests that this promising lead-free material is characterised, for instance, by the piezoelectric coefficients d_{33} = 380 pC/N (longitudinal) and d_{15} = 690 pC/N (shear), which are larger than the similar constants of the conventional PZT-5 or PZT-5A FC[15,18] based on Pb(Zr, Ti)O_3. The longitudinal electromechanical coupling factor (ECF) of the poled KNNS–BNZH FC is $k_{33} = 0.70$,[18] and this parameter equals k_{33} of the PZT-5A FC.[18] In this context, the KNNS–BNZH FC may be of value as a piezoelectric component of novel lead-free composites. Below we show how the KNNS–BNZH FC influences the piezoelectric performance and related parameters of the 0–3 and 0–3–0 composites. The aim of this paper is to analyse piezoelectric sensitivity, ECFs and related FOMs of novel 0–3-type composites with prolate KNNS–BNZH FC inclusions.

2. 0–3-Type Composites and their Performances

2.1. *Model and effective parameters*

The composite represents a system of the FC inclusions arranged in a large polymer matrix (Fig. 1). The shape of each FC inclusion is described by the equation $(x_1/a_1)^2 + (x_2/a_2)^2 + (x_3/a_3)^2 = 1$ in the coordinate system $(X_1X_2X_3)$, where $a_1 = a_2$. The remanent polarisation of each FC inclusion is $\boldsymbol{P}_r^{(1)} \parallel OX_3$. It is assumed that centres of these FC inclusions occupy the sites of a simple tetragonal lattice with unit-cell vectors being parallel to the OX_k axes shown in Fig. 1. To characterise the shape of the FC inclusion, we introduce the aspect ratio $\rho = a_1/a_3$. The polymer matrix surrounding the FC inclusions is either monolithic (inset 1 in Fig. 1) or porous (inset 2 in Fig. 1). The shape of each isolated pore is described by the equation $(x_1/a_{1,p})^2 + (x_2/a_{2,p})^2 + (x_3/a_{3,p})^2 = 1$, where $a_{1,p} = a_{2,p}$, and the aspect ratio of the pore is $\rho_p = a_{1,p}/a_{3,p}$. Centres of the pores in the polymer medium occupy the sites of a simple tetragonal lattice with unit-cell vectors that are parallel to the OX_k axes in Fig. 1 (by analogy with the arrangement of tbe FC inclusions), and the linear sizes of each pore are much smaller than the smallest axis of the spheroidal FC inclusion. We also assume that surface charges appearing owing to the ferroelectric polarisation of each FC inclusion are fully screened by free charge carriers flowing to interfaces between the components of the composite. The composite (Fig. 1) with the monolithic matrix is characterised by 0–3 connectivity in terms of work,[4,19] and the composite with the porous matrix is characterised by 0–3–0 connectivity.

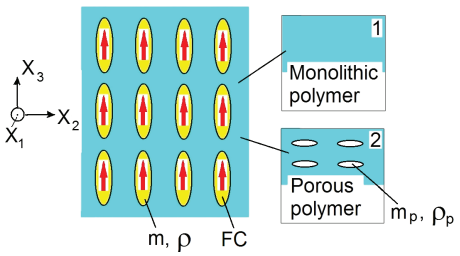

Fig. 1. Schematic of the 0–3-type composite. $(X_1X_2X_3)$ is a rectangular coordinate system, m is the volume fraction of FC, ρ is the aspect ratio of the FC inclusion, m_p is the volume fraction of air pores in the polymer matrix and ρ_p is the aspect ratio the air pore. The arrow shows the orientation of the remanent polarisation vector in the FC inclusion.

The effective electromechanical properties of the 0–3 composite are evaluated by means of the effective field method (EFM).[4,20] In the EFM, an electromechanical interaction between the aligned piezoelectric inclusions is taken into account in terms of the effective electroelastic field that acts on each FC inclusion in the composite. The effective properties determined for the 0–3 composite by using the EFM are given by

$$\| \boldsymbol{C}^* \| = \| \boldsymbol{C}^{(2)} \| + m\,(\| \boldsymbol{C}^{(1)} \| - \| \boldsymbol{C}^{(2)} \|)\cdot[\| \boldsymbol{I} \| + (1-m)\times \| \boldsymbol{S} \| \cdot \| \boldsymbol{C}^{(2)} \|^{-1}\cdot(\| \boldsymbol{C}^{(1)} \| - \| \boldsymbol{C}^{(2)} \|)]^{-1}. \quad (1)$$

The $\| \boldsymbol{C}^* \|$ matrix from Eq. (1) is written in the general form as follows:

$$\| \boldsymbol{C}^* \| = \begin{pmatrix} \| \boldsymbol{c}^{*E} \| & \| \boldsymbol{e}^* \|^t \\ \| \boldsymbol{e}^* \| & -\| \varepsilon^{*\xi} \| \end{pmatrix}, \quad (2)$$

In Eq. (1) $\| \boldsymbol{C}^{(1)} \|$ and $\| \boldsymbol{C}^{(2)} \|$ describe the electromechanical properties of the inclusion and surrounding medium, respectively, $\| \boldsymbol{I} \|$ is the identity matrix, and $\| \boldsymbol{S} \|$ is the matrix that contains the electroelastic Eshelby tensor components[21] that depend on the elements of $\| \boldsymbol{C}^{(2)} \|$ and on the aspect ratio ρ of the inclusion. In Eq. (2) $\| \boldsymbol{c}^{*E} \|$, $\| \boldsymbol{e}^* \|$ and $\| \boldsymbol{e}^{*\xi} \|$ characterise elastic moduli at E = const, piezoelectric coefficients and dielectric permittivities of the composite at ξ = const, respectively, and the superscript t is used to show the transposition of the matrix. The $\| \boldsymbol{C}^{(1)} \|$ and $\| \boldsymbol{C}^{(2)} \|$ matrices from Eq. (1) have the structure of the $\| \boldsymbol{C}^* \|$ matrix from Eq. (2).

In a case of the 0–3–0 connectivity pattern, the $\| \boldsymbol{C}^{(2)} \|$ matrix related to the porous polymer medium is to be found before averaging in accordance with Eq. (1). The effective properties of the porous polymer medium are found by using the method,[22] and the main formula has the form

$$\| \boldsymbol{C}^{(2)} \| = \| \boldsymbol{C}_p \| \cdot [\| \boldsymbol{I} \| - m_p(\| \boldsymbol{I} \| - (1-m_p) \| \boldsymbol{S}_p \|)^{-1}], \quad (3)$$

where $\| \boldsymbol{C}_p \|$ characterises the properties of polymer, $\| \boldsymbol{S}_p \|$ contains the Eshelby tensor components,[21] and these tensor components depend on the $\| \boldsymbol{C}_p \|$ elements and aspect ratio ρ_p of the pore.

In the final stage of our study, we compare the effective parameters evaluated by using the EFM [see Eq. (1)] to the effective parameters evaluated by means of the effective medium method (EMM)[4,20] that is also termed "self-consistent method." In the EMM, it is assumed that a single piezoelectric inclusion is surrounded by an effective piezoelectric medium, and this medium represents a matrix with the similar inclusions. The effective electromechanical properties

are evaluated by taking into account the electromechanical interaction between the aforementioned single inclusion and surrounding medium. In the EMM, the matrix of the effective properties of the composite is written as follows:

$$\| \boldsymbol{C}^* \| = \| \boldsymbol{C}^{(2)} \| + m (\| \boldsymbol{C}^{(1)} \| - \| \boldsymbol{C}^{(2)} \|) \cdot \| \boldsymbol{A} \|, \quad (4)$$

where

$$\| \boldsymbol{A} \| = [\| \boldsymbol{I} \| + \| \boldsymbol{S} \| \cdot \| \boldsymbol{C}^* \|^{-1} \cdot (\| \boldsymbol{C}^{(1)} \| - \| \boldsymbol{C}^* \|)]^{-1}, \quad (5)$$

is the mechanical strain – electric field concentration matrix.[20] In Eq. (5), the $\| \boldsymbol{C}^* \|$ matrix characterises the effective properties of the composite (as an effective medium surrounding the inclusion), and the $\| \boldsymbol{C}^* \|$ matrix from Eq. (5) equals $\| \boldsymbol{C}^* \|$ from Eq. (4). The procedure to be carried out in the EMM is self-consistent[4,20] and needs iterations for solving Eq. (4) and evaluating the effective properties of the composite. In a case of the 0–3–0 composite, the $\| \boldsymbol{C}^{(2)} \|$ matrix is related to the porous polymer medium with the properties determined previously within the framework of Eq. (3). The final $\| \boldsymbol{C}^* \|$ matrix from Eq. (4) has the structure shown in Eq. (2).

The effective properties of the 0–3 composite and elements of $\| \boldsymbol{C}^* \|$ from Eqs. (1), (2) and (4) depend on the volume fraction m and aspect ratio ρ of the FC inclusions (Fig. 1). Taking into account porosity of the polymer matrix (see inset 2 in Fig. 1), we note that the effective properties of the 0–3–0 composite depend on m, ρ, m_p, and ρ_p. A transition from the full set of electromechanical constants involved in Eq. (2) to the piezoelectric coefficients d_{ij}^* and g_{ij}^*, elastic compliances s_{ab}^{*E}, and dielectric permittivities $\varepsilon_{pp}^{*\sigma}$ at mechanical stress $\sigma = \text{const}$ is performed in terms of formulae[23] for a piezoelectric medium.

In this paper, we analyse the following effective parameters of the lead-free 0–3-type composites:

(i) piezoelectric coefficients

$$g_{3j}^* = d_{3j}^* / \varepsilon_{33}^{*\sigma}, \quad (6)$$

(ii) traditional (or squared) FOMs

$$(Q_{3j}^*)^2 = d_{3j}^* g_{3j}^*, \quad (7)$$

(iii) ECFs

$$k_{3j}^* = d_{3j}^* / (\varepsilon_{33}^{*\sigma} \; s_{jj}^{*E})^{1/2}, \quad (8)$$

and (iv) modified FOMs for a stress-driven harvester

$$F_{3j}^{*\sigma} = L_{3j}^* (Q_{3j}^*)^2, \quad (9)$$

where

$$L_{3j}^* = [(k_{3j}^*)^{-1} - ((k_{3j}^*)^{-2} - 1)^{1/2}]^2 / (k_{3j}^*)^2, \quad (10)$$

and $j = 1$ and 3. The piezoelectric coefficients g_{3j}^* from Eq. (6) characterise the sensitivity[4,15,16] of a piezoelectric sample, its ability to generate an electric field under an external mechanical stress. The FOMs $(Q_{3j}^*)^2$ from Eq. (7) characterise the sensing and actuating capability of the piezoelectric coefficient and are used to describe the " signal / noise" ratio and energy-harvesting performance.[4,15,24] The ECFs k_{3j}^* from Eq. (8) describe an effectiveness of the energy conversion in the piezoelectric medium.[4,23] The modified FOMs $F_{3j}^{*\sigma}$ from Eq. (9) are important[24] to describe an effectiveness of a piezoelectric material in the sense of ability to convert input mechanical energy to useable electrical energy at $\sigma = \text{const}$. In Eq. (10), the ECF k_{3j}^* is considered as an absolute value. The modified FOMs L_{3j}^* from Eq. (10) are used to evaluate the "maximum output electrical energy/stored electrical energy" ratio[24] for the piezoelectric sample.

In this paper, we analyse the effective parameters (6)–(9) of the 0–3-type composites wherein the poled KNNS–BNZH FC is the piezoelectric component, and high-density polyethylene is the piezo-passive component. Experimental constants of these components[18,25] are shown in Table 1. As follows from Table 1, the KNNS–BNZH FC exhibits the small anisotropy of both the piezoelectric coefficients ($e_{33} / | e_{33} | \approx 1.4$) and dielectric permittivities ($\varepsilon_{11}^{*\xi} / \varepsilon_{33}^{*\xi} \approx 1.1$).

2.2. *Volume-fraction and aspect-ratio dependences of effective parameters*

In Sec. 2.2, we show and analyse some examples of the volume-fraction (m) and aspect-ratio (ρ) dependences of the effective parameters (6)–(9) which are evaluated for the 0–3 KNNS–BNZH FC / polyethylene composite and 0–3–0 KNNS–BNZH FC / porous polyethylene composite.

2.2.1. *0–3 Composite*

Graphs of the effective parameters of the 0–3 composite based on the KNNS–BNZH FC are shown in Fig. 2. It is seen that the piezoelectric coefficients g_{3j}^* from Eq. (6), FOMs $(Q_{3j}^*)^2$ and $F_{3j}^{*\sigma}$ from Eqs. (7) and (9), and ECFs k_{3j}^* from Eq. (8) strongly depend on the volume fraction of FC m and aspect ratio of the FC inclusion ρ at $m << 1$ and $\rho << 1$. To describe

Table 1. Room-temperature elastic moduli c_{ab}^E (in 10^{10} Pa), piezoelectric coefficients e_{ij} (in C / m^2) and dielectric permittivity ε_{pp}^{ξ} of FC and polymer components.

Components	c_{11}^E	c_{12}^E	c_{13}^E	c_{33}^E	c_{44}^E	e_{31}	e_{33}	e_{15}	$e_{11}^{\xi}/\varepsilon_0$	$e_{33}^{\xi}/\varepsilon_0$
KNNS–BNZH FC[18]	13.62	8.62	6.59	9.85	2.28	–11.2	15.9	15.6	1100	975
Polyethylene[15,24]	0.0778	0.0195	0.0195	0.0778	0.0292	0	0	0	2.3	2.3

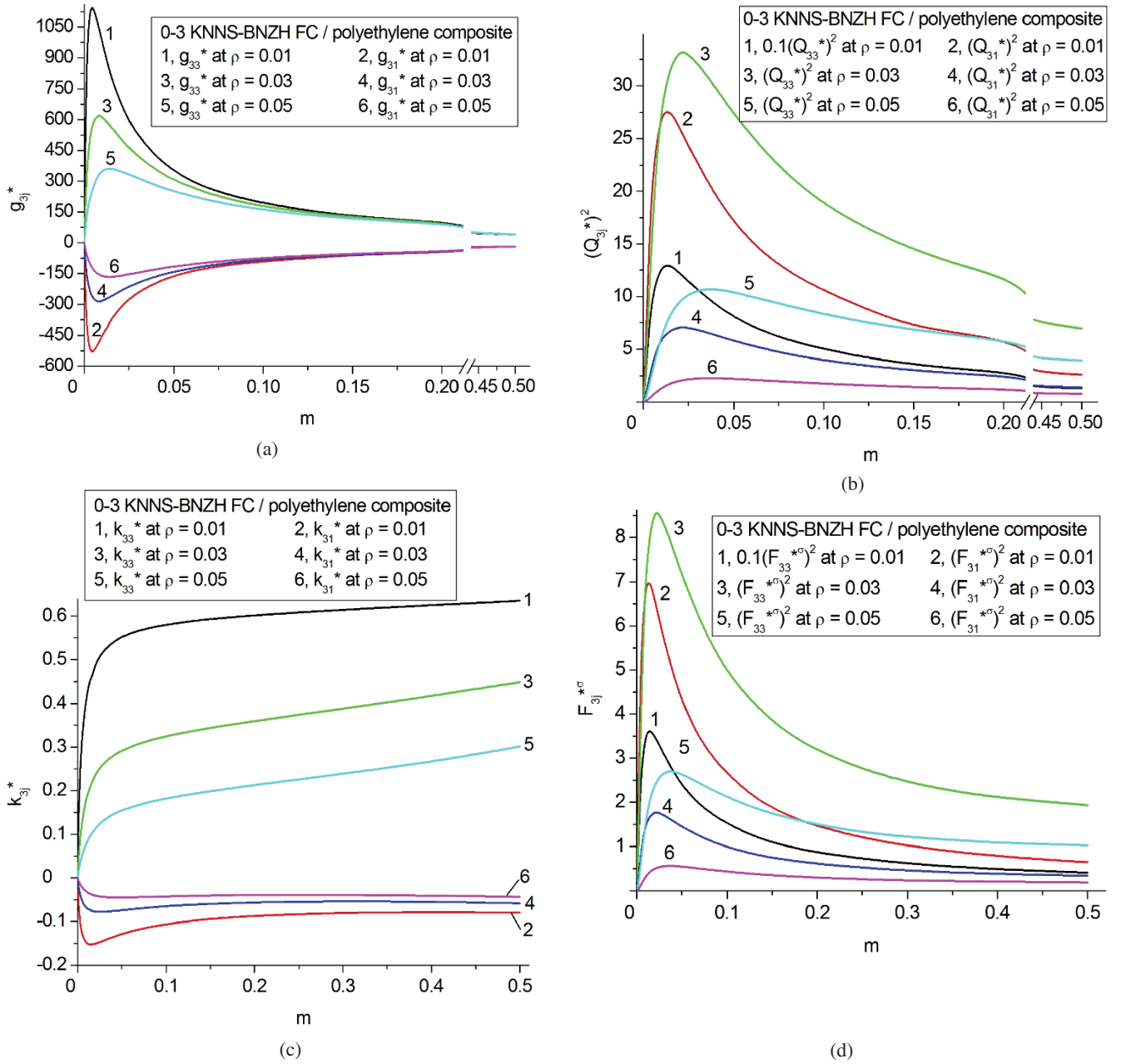

Fig. 2. Volume-fraction (m) dependences of effective piezoelectric coefficients g_{3j}^* (a, in mV·m/N), squared FOMs $(Q_{3j}^*)^2$ (b, in 10^{-12} Pa^{-1}), ECFs k_{3j}^* (c), and modified FOMs $F_{3j}^{*\sigma}$ (d, in 10^{-12} Pa^{-1}) of the 0–3 KNNS–BNZH FC / polyethylene composite at ρ = const. Effective electromechanical properties of the composite are found by means of the EFM, see Eq. (1).

the performance of the 0–3-type composites in this work, we consider the ranges of $0.001 \le m < 0.5$ and $0.01 \le \rho \le 0.15$.

The system of the very prolate FC inclusions with $\rho << 1$ (Fig. 1) promotes the larger piezoelectric coefficients d_{33}^* and g_{33}^* of the 0–3 composite at m = const. The presence of extreme points of g_{3j}^* at $m << 1$ (Fig. 2(a) is accounted for by the active influence of the dielectric permittivity $\varepsilon_{33}^{*\sigma}$ of the composite at $\varepsilon_{33}^{*\sigma} \sim \varepsilon_{33}^{(2),\sigma}$ in the volume-fraction region of $m << 1$. Increasing the aspect ratio ρ of the FC inclusion at m = const leads to the smaller $| d_{3j}^* |$ values, and hence, stimulates decreasing $| g_{3j}^* |$ in accordance with Eq. (6). Such a feature of the 0–3 composite is associated with specifics of its piezoelectric activity in the presence of the isolated FC inclusions (Fig. 1). The next important feature of the 0–3 composite consists in the almost constant volume fractions m related to max g_{33}^* and min g_{31}^* (see, for instance, curves 1 and 2 in Fig. 2(a)).

The larger piezoelectric coefficients d_{3j}^* and g_{3j}^* lead to the larger FOMs $(Q_{3j}^*)^2$ from Eq. (7). Increasing the aspect ratio ρ leads to the larger volume fraction m at which points

of max$[(Q_{3j}^*)^2]$ are observed (Fig. 2(b), and the maximum sharpness is weakened. The latter feature is associated with the smaller piezoelectric coefficients $|\, d_{3j}^* \,|$ and $|\, g_{3j}^* \,|$ of the composite at the larger aspect ratio ρ and m = const. Comparison of curves 2 and 3 or curves 4 and 6 in Fig. 2(b) enables us to assert that the aspect-ratio influence on FOMs $(Q_{3j}^*)^2$ is strong even in the narrow aspect-ratio range, e.g., at $0.01 \le \rho \le 0.05$.

As follows from the volume-fraction dependence of the ECFs k_{3j}^* from Eq. (8), a weak minimum of k_{31}^* is the only example of the non-monotonic behaviour shown in Fig. 2(c). The presence of min k_{31}^* at $0.01 \le \rho \le 0.04$ is accounted for a link between k_{31}^* and g_{31}^*. Taking into account Eqs. (6) and (8), we write the ECF $k_{31}^* = g_{31}^* (\varepsilon_{33}^{*\sigma} / s_{11}^{*E})^{1/2}$ and show that the proportionality $k_{31}^* \sim g_{31}^*$ is more pronounced at the smaller aspect ratio ρ. The ECF $k_{33}^* = g_{33}^* (\varepsilon_{33}^{*\sigma} / s_{33}^{*E})^{1/2}$ exhibits the monotonic behaviour (see curves 1, 3 and 5 in Fig. 2(c)) even despite the presence of max g_{33}^* (see curves 1, 3 and 5 in Fig. 2(a)). Such a behaviour is concerned with the strong influence of the $\varepsilon_{33}^{*\sigma} / s_{33}^{*E}$ ratio on the $k_{33}^*(m)$ dependence. It is obvious that the $\varepsilon_{33}^{*\sigma} / s_{33}^{*E}$ ratio can influence the longitudinal piezoelectric effect and ECF k_{33}^* to a larger extent due to the very prolate shape of the FC inclusions oriented along the poling axis (Fig. 1). In contrast to $\varepsilon_{33}^{*\sigma} / s_{33}^{*E}$, the $\varepsilon_{33}^{*\sigma} / s_{11}^{*E}$ ratio is less sensible to changes in the aspect ratio ρ and/or volume fraction m of the FC inclusions because of specifics of the dielectric and elastic response of the studied 0–3 composite.

Comparing Figs. 2(b)–2(d) and considering Eq. (9), we note the important analogy between the $[Q_{3j}^*(m)]^2$ and $F_{3j}^{*\sigma}(m)$ dependences. This analogy is achieved due to the stable behaviour of $L_{3j}^*(m)$. Maxima of $F_{3j}^{*\sigma}(m)$ shift towards the larger volume fractions m in comparison to max $[Q_{3j}^*(m)]^2$ or max g_{33}^*, and this is important to take into account on manufacturing the composite.[14–16]

In general, one can note that the volume-fraction range of $0 < m < 0.2$ is of interest to achieve the large g_{33}^*, $(Q_{33}^*)^2$ and $F_{33}^{*\sigma}$ values (Figs. 2(a), 2(b) and 2(d)) at the aspect ratio $\rho << 1$. These effective parameters remain relatively large even on increasing the volume fraction m by 0.05–0.10. The large k_{33}^* values are achieved at $m > 0.1$ owing to the monotonic increase of $k_{33}^*(m)$ (Fig. 2(d) irrespective of ρ. An anisotropy of g_{3j}^*, $(Q_{3j}^*)^2$ and $F_{3j}^{*\sigma}$ undergoes minor changes in the range of $0 < m < 0.2$ at $\rho << 1$.

An example of the aspect-ratio (ρ) dependence of the effective parameters (6), (7) and (9) of the 0–3 composite is shown in Fig. 3(a). We observe this dependence at the volume fraction $m = 0.1$ that is related to large values of g_{33}^*, $(Q_{33}^*)^2$ and $F_{33}^{*\sigma}$. However these values decrease markedly on increasing ρ from 0.01 to 0.10, and this is concerned with the key role of the prolate shape of the FC inclusion in forming the piezoelectric properties of the composite. A further increase of ρ does not lead to the significant decrease of $(Q_{33}^*)^2$ and $F_{33}^{*\sigma}$, and these parameters at $\rho > 0.10$ are small in comparison to those at $\rho = 0.01$. Thus, we emphasise the

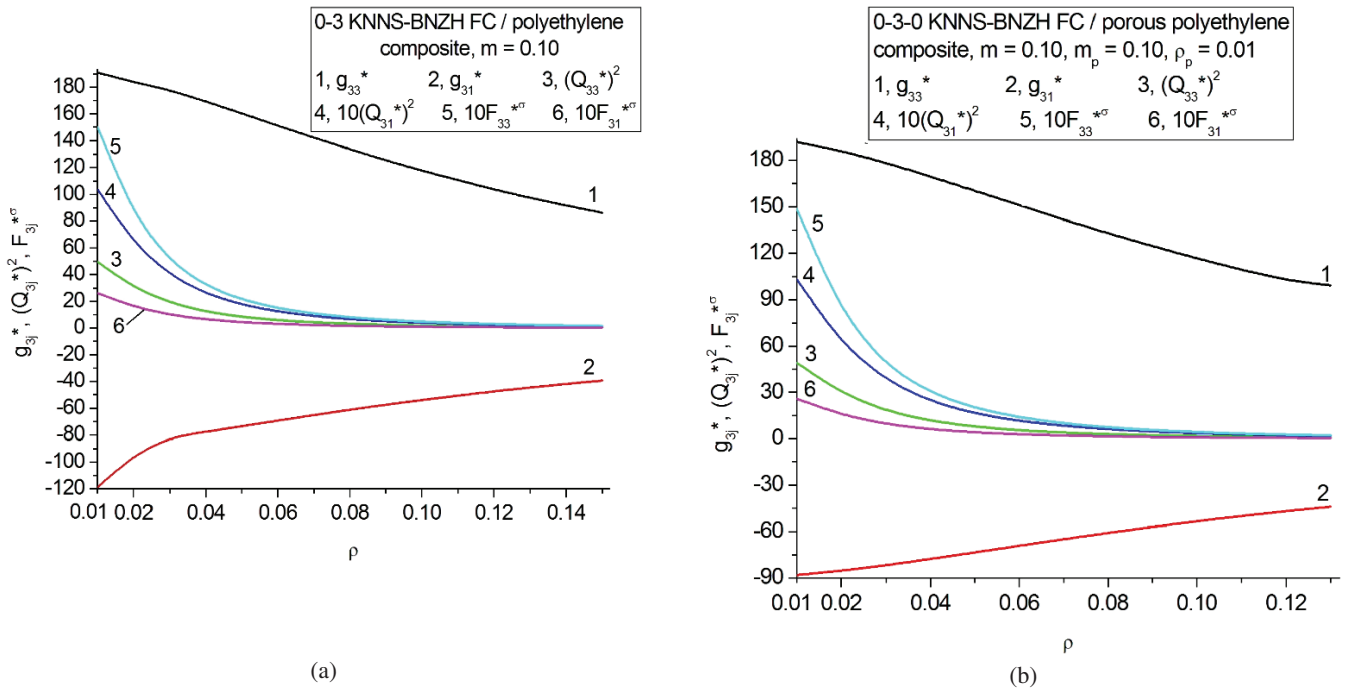

(a) (b)

Fig. 3. Aspect-ratio (ρ) dependences of effective piezoelectric coefficients g_{3j}^* (in mV·m/N), squared FOMs $(Q_{3j}^*)^2$ (in 10^{-12} Pa^{-1}) and modified FOMs $F_{3j}^{*\sigma}$ (in 10^{-12} Pa^{-1}) of the 0–3 KNNS–BNZH/polyethylene composite (a) and 0–3–0 KNNS–BNZH / porous polyethylene composite (b–e). Effective electromechanical properties of the composites are found by means of the EFM [see Eq. (1)], and properties of the porous polymer matrix are determined in accordance with Eq. (3).

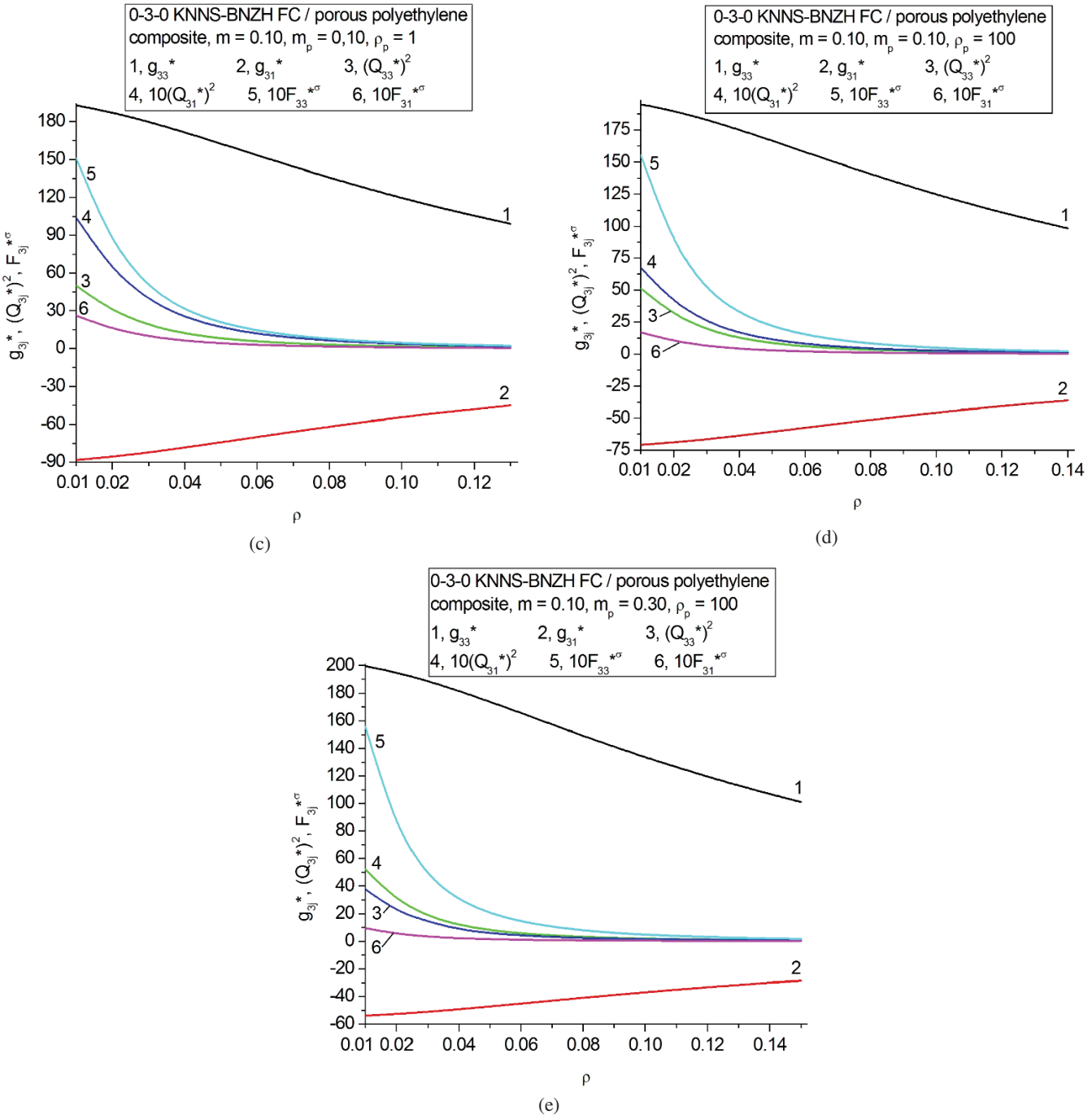

Fig. 3. (*Continued*)

strong influence of the microgeometrical factor (namely, the aspect ratio ρ of the FC inclusion) on the piezoelectric performance and FOMs of the 0–3 composite based on the KNNS–BNZH FC.

2.2.2. *0–3–0 Composites*

Graphs in Figs. 3(b)–3(e) show examples of the aspect-ratio behaviour of the effective parameters (6), (7) and (9) of the 0–3–0 composite at the volume fraction of FC $m = 0.10$. Now we change characteristics of the matrix that surrounds the FC inclusions in the composite, see inset 2 in Fig. 1. Among these characteristic we mention the volume fraction of pores (or porosity) m_p and aspect ratio of pores ρ_p. Comparing graphs in Figs. 3(b)–3(d), we note changes in the effective parameters of the 0–3–0 composite at the relatively small porosity $m_p = 0.10$. Hereby, the aspect ratio of each pore in the polymer medium undergoes changes from $\rho_p = 0.01$ (highly

prolate pore) to $\rho_p = 100$ (highly oblate pore), cf. Figs. 3(b) and 3(d). These changes mainly lead to decreasing $|\, g_{31}^{*}\,|$, $(Q_{31}^{*})^2$ and $F_{31}^{*\sigma}$ which are concerned with the transverse piezoelectric effect. Case of $\rho_p = 1$, that is related to the spherical air pore shape in the polymer medium, may be regarded as an intermediate on comparing the effective parameters in Figs. 3(b)–3(d). As noted for the 0–3 composite (see Sec. 2.2.1), at $\rho > 0.10$ the effective parameters (6), (7) and (9) of the 0–3–0 composite become small in comparison to the similar parameters at $\rho = 0.01$, and such a trend is observed irrespective of ρ_p. We again see the strong influence of the aspect ratio of the FC inclusions ρ on the effective parameters of the 0–3–0 composite by analogy with that described in the final part of Sec. 2.2.1.

Our further description in Sec. 2.2.2 concerns Figs. 3(d) and 3(e). Increasing porosity from $m_p = 0.10$ (Fig. 3(d) to in both these cases) enables us to improve the piezoelectric sensitivity, anisotropy and related parameters of the composite. On increasing porosity m_p the piezoelectric coefficient g_{33}^{*} and FOM $(Q_{33}^{*})^2$ increase to a certain extent at $m << 1$ (see curves 1 and 3 in Figs. 3(d) and 3(e)), however the modified FOM $F_{33}^{*\sigma}$ undergoes minor changes (see curve 5 in Figs. 3(d) and 3(e)). In our opinion, the larger g_{33}^{*} and $(Q_{33}^{*})^2$ values in Fig. 3(e) are caused by the smaller dielectric permittivity of the composite $\varepsilon_{33}^{*\sigma}$ at $m_p = 0.30$ in comparison to $\varepsilon_{33}^{*\sigma}$ of the similar composite at $m_p = 0.10$, $\rho_p = 100$, $m = \text{const}$, and $\rho = \text{const}$. Comparing Figs. 3(d) and 3(e), we observe decreasing $|\, g_{31}^{*}\,|$, $(Q_{31}^{*})^2$ and $F_{31}^{*\sigma}$. Both the larger porosity m_p and highly oblate pores at $\rho_p >> 1$ weaken the transverse piezoelectric effect in the 0–3–0 composite to a certain degree and, therefore, influence the anisotropy of the effective parameters of this composite.

2.3. *New diagrams*

In Sec. 2.3, we put forward $\rho - m$ diagrams that are plotted for the 0–3 composite (Fig. 4(a) and 0–3–0 composite (Fig. 4(b) for the first time. In both the diagrams we show regions 1 and 2 which are related to validity of conditions

$$g_{33}^{*} > 100 \text{ mV·m/N} \quad \text{and} \quad F_{33}^{*\sigma} > F_{33}^{(1),\sigma}, \tag{11}$$

respectively. Inequalities (11) mean the high longitudinal piezoelectric sensitivity of the composite in comparison to the longitudinal sensitivity of its FC component (i.e., $g_{33}^{*}/g_{33}^{(1)} > 4.8$) and the large modified FOM related to the longitudinal piezoelectric response. It is shown that regions 1 and 2 do not undergo significant changes on replacing the monolithic polymer with the porous polymer at $\rho >> 1$. In Fig. 4(b), region 3 means that the condition for the large anisotropy of the modified FOMs

$$F_{33}^{*\sigma}/F_{31}^{*\sigma} > 10 \tag{12}$$

holds for the 0–3–0 composite with the polymer matrix containing the highly oblate air pores. Such a porous polymer

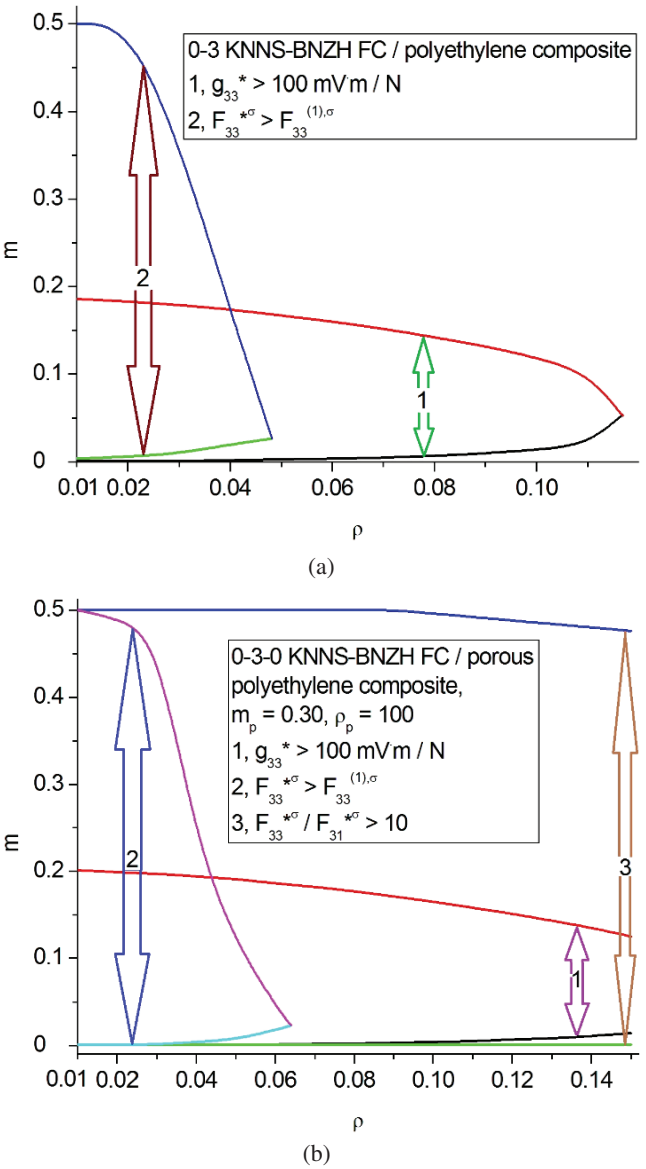

Fig. 4. Diagrams that show regions of the large piezoelectric coefficient g_{33}^{*}, modified FOM $F_{33}^{*\sigma}$ and anisotropy $F_{33}^{*\sigma}/F_{31}^{*\sigma}$ which are found for the 0–3-type KNNS–BNZH-based composites. Effective electromechanical properties of the composites are found by means of the EFM [see Eq. (1)], and properties of the porous polymer matrix are determined in accordance with Eq. (3).

matrix is characterised by the large elastic anisotropy[26] that promotes the better longitudinal piezoelectric sensitivity and weakens the transverse piezoelectric response of the composite sample in the wide volume-fraction (m) range. It is noteworthy that the m range in region 3 (Fig. 4(b) remains relatively wide and almost constant at $0.01 \le \rho \le 0.15$. However, it should be added that the modified FOM $F_{33}^{*}\sigma$ decreases rapidly on increasing the aspect ratio ρ (see curve 5 in Fig. 3(e)), and in the sense of potential applications, the aspect ratios from the range of $0.01 \le \rho \le 0.05$ would be preferable.

Table 2. Comparison of effective piezoelectric coefficients evaluated for the 0–3 KNNS–BNZH FC / polyethylene composite by means of the EFM and EMM.[a]

ρ	m	d_{33}^*, pC / N	d_{31}^*, pC / N	g_{33}^*, mV·m / N	g_{31}^*, mV·m / N
0.01	0.05	231 (236)	–106 (–109)	350 (362)	–161 (–167)
	0.10	259 (271)	–119 (–122)	191 (202)	–87.5 (–90.8)
	0.30	295 (329)	–133 (–148)	67.6 (71.3)	–30.5 (–32.1)
0.05	0.05	41.5 (42.6)	–19.1 (–19.5)	251 (260)	–115 (–119)
	0.10	51.9 (56.0)	–23.8 (–25.0)	160 (163)	–73.4 (–75.0)
	0.30	73.2 (80.8)	–33.0 (–36.5)	64.4 (67.1)	–29.0 (–30.3)
0.10	0.05	11.2 (11.4)	–5.12 (–5.20)	147 (153)	–67.4 (–69.8)
	0.10	16.0 (16.6)	–7.29 (7.34)	118 (123)	–53.8 (–54.5)
	0.30	26.5 (29.2)	–11.9 (12.9)	58.5 (60.9)	–26.3 (–26.9)

Note: [a]Results obtained by means of the EMM are given in parentheses.

3. Comparison of Results and Discussion

In Sec. 2, we analysed examples of the high piezoelectric sensitivity, large FOMs and anisotropy of some parameters of the lead-free 0–3-type composites. The effective electromechanical properties of these composites were evaluated by using the EFM, and the related parameters were found by taking into account the EFM results. Now, we compare some parameters calculated by means of two methods, namely, the EFM and EMM. Table 2 shows results on the piezoelectric coefficients d_{3j}^* and g_{3j}^* which were evaluated by means of the EFM [see Eq. (1)] and by using the EMM [see Eqs. (4) and (5)]. We see the similar volume-fraction (m) and aspect-ratio (ρ) dependences in Table 2. A difference between the piezoelectric coefficients d_{3j}^* evaluated by using these two methods increases on increasing m at ρ = const or on decreasing ρ at m = const. Both the modes of changing m and ρ lead to an increase of the piezoelectric activity, i.e., to the larger $| d_{3j}^* |$ values of the 0–3 composite.

In contrast to the piezoelectric coefficients d_{3j}^*, a difference between the piezoelectric coefficients g_{3j}^* evaluated by using the EFM and EMM decreases at the same modes of changing m and ρ, see Table 2. This may be concerned with specifics of the determination of the dielectric permittivity $\varepsilon_{33}^{*\sigma}$ in these methods and with the important link between the piezoelectric coefficients d_{3j}^* and g_{3j}^*, see Eq. (6).

The volume-fraction and aspect-ratio dependences shown in Table 2 have trends being similar to those in a 0–3 PMN–0.33PT single crystal / araldite composite[27] with spheroidal aligned inclusions. Despite the very large piezoelectric coefficients d_{3j} of the domain-engineered PMN–0.33PT single crystal ($d_{3j} \sim 10^3$ pC / N)[4,26] in comparison to the d_{3j} values of the KNNS–BNZH FC,[18] we find comparable values of two parameters related to the 0–3 KNNS–BNZH-based and PMN–0.33PT-based composites with the similar microgeometry. These parameters are the longitudinal piezoelectric coefficient g_{33}^* and ECF k_{33}^* at the aspect ratio $\rho = 0.1$.

The piezoelectric coefficients of the studied KNNS–BNZH-based composites (see, e.g., data in Table 2) are larger than the same parameters found[28] for advanced lead-free FC/epoxy composites with well-ordered 3–1 and 3–2 channel structures. According to experimental results[28] on the 3–1 and 3–2 $(Na_{0.5}K_{0.5})NbO_3$ / epoxy composites, largest values of their longitudinal piezoelectric coefficients are $d_{33}^* = 98$ pC / N and $g_{33}^* = 66$ mV·m / N. The largest g_{33}^* value of a $(K_{0.50}Na_{0.50})_{0.94}Li_{0.06}NbO_3$ FC / epoxy composite[29] structured through the dielectrophoresis is 118 mV·m/N, and the largest g_{33}^* value related to a quasi 1–3 dielectrophoretically structured $K_{0.485}Na_{0.485}Li_{0.03}NbO_3$ FC / polydimethylsiloxane composite[9] equals 510 mV·m / N. The same quasi 1–3 composite is characterised[9] by the largest FOM $(Q_{33}^*)^2 = 17.9 \cdot 10^{-12}$ Pa^{-1}. The aforementioned g_{33}^* and $(Q_{33}^*)^2$ values from Refs. 9 and 29 are comparable to those of the studied 0–3 KNNS–BNZH-based composite at the volume fraction of FC $m \approx 0.1$ (see Figs. 2(a) and 2(b)).

4. Conclusions

This paper reports new results on the piezo-active lead-free 0–3-type composites based on the KNNS–BNZH FC[18] with the relatively large piezoelectric coefficients d_{3j}. The non-monotonic volume-fraction (m) dependences of the effective piezoelectric coefficients g_{3j}^*, ECF k_{31}^*, FOMs $(Q_{3j}^*)^2$, and modified FOMs $F_{3j}^{*\sigma}$ (Fig. 2) have been analysed. The new diagrams (Fig. 4) show regions of validity of conditions (11) and (12) in terms of the m and ρ ranges related to the 0–3-type composites.

The system of highly prolate FC inclusions oriented along the poling axis OX_3 (see Fig. 1) promotes the large parameters of the studied composites (see Figs. 2–4 and Table 2) and make them competitive among piezo-active composites[9,14–16,26–29] including modern lead-free composites. The oblate air pores in the polymer matrix (see inset 2 in Fig. 1) help to weaken the transverse piezoelectric response of the

0–3–0 composite, and this weakening leads to the large anisotropy of d_{3j}^*, g_{3j}^*, $(Q_{3j}^*)^2$, and $F_{3j}^{*\sigma}$. The large anisotropy of d_{3j}^* and g_{3j}^* at the piezoelectric coefficient $g_{33}^* >$ 100 mV·m / N can promote sensor applications concerned with an exploitation of the longitudinal oscillation mode. The large FOM $(Q_{33}^*)^2$ values (about 10^{-10} Pa^{-1}) are important for energy-harvesting and sensor applications where the longitudinal piezoelectric response plays the key role. The large modified FOM $F_{33}^{*\sigma}$ (about 10^{-11} Pa^{-1}) are to be effective in stress-driven piezoelectric devices or systems.

Acknowledgments

This paper is performed within the framework of the programme supporting publication activity of the Southern Federal University. The authors would like to thank Prof. Dr. I. A. Parinov and Prof. Dr. A. E. Panich (Southern Federal University, Russia), and Prof. Dr. C. R. Bowen (University of Bath, UK) for their interest in the field of modern piezoelectric materials, their performance and applications.

References

[1]E. K. Akdogan, M. Allahverdi and A. Safari, Piezoelectric composites for sensor and actuator applications, *IEEE Trans. Ultrason. Ferroelectr. Freq. Control* **52**, 746 (2005).

[2]F. Wang, C. He and Y. Tang, Single crystal 0.7Pb($Mg_{1/3}Nb_{2/3}$)-O_3–0.3$PbTiO_3$/epoxy 1–3 piezoelectric composites prepared by the lamination technique, *Mater. Chem. Phys*. **105**, 273 (2007).

[3]K. Ren, Y. Liu, X. Geng, H. F. Hofmann and Q. M. Zhang, Single crystal PMN–PT / epoxy 1–3 composite for energy-harvesting application, *IEEE Trans. Ultrason. Ferroelectr. Freq. Control* **53**, 631 (2006).

[4]V. Yu. Topolov and C. R. Bowen, *Electromechanical Properties in Composites Based on Ferroelectrics* (Springer, London, 2009).

[5]I. Coondoo, N. Panwar and A. Kholkin, Lead-free piezoelectrics: Current status and perspectives, *J. Adv. Dielect*. **3**, 1330002 (2013).

[6]C.-H. Hong, H.-P. Kim, B.-Y. Ghoi, H.-S. Han, J.-S. Son, C.W. Ahn and W. Jo, Lead-free piezoceramics — Where to move on?, *J. Materiomics* **2**, 1 (2016).

[7]D. Maurya, M. Peddigari, L. D. Geng, N. Sharpes, V. Annapureddy, H. Palneedi, R. Sriramdas, Y. Yan, H.-C. Song, Y. U. Wang, J. Ryu and S. Priya, Lead-free piezoelectric materials and composites for high power density energy harvesting, *J. Mater. Res*. **33**, 2235 (2018).

[8]D. Zhou, K. H. Lam, Yan Chen, Q. Zhang, Y. C. Chiu, H. Luo, J. Dai and H. L. W. Chan, Lead-free piezoelectric single crystal based 1–3 composites for ultrasonic transducer applications, *Sens. Actuators A Phys.* **182**, 95 (2012).

[9]V. L. Stuber, D. B. Deutz, J. Bennett, D. Cannel, D. M. de Leeuw, S. van der Zwaag and P. Groen, Flexible lead-free piezoelectric composite materials for energy harvesting applications, *Energy Technol.* **7,** 177 (2019).

[10]V. Yu. Topolov, A. N. Isaeva and P. Bisegna, Novel lead-free composites with two porosity levels: Large piezoelectric anisotropy and high sensitivity, *J. Phys. D Appl. Phys*. **53**, 395303 (2020).

[11]V. Yu. Topolov, C. R. Bowen and A. N. Isaeva, Anisotropy factors and electromechanical coupling in lead-free 1–3-type composites, *IEEE Trans. Ultrason. Ferroelectr. Freq. Control* **65**, 1278 (2018).

[12]S. A. Riquelme and K. Ramam, Dielectric and piezoelectric properties of lead free BZT-BCT/PVDF flexible composites for electronic applications, *Mater. Res. Express* **6**, 116331 (2019).

[13]S. Qian, L. Qin, J. He, X. Niu, J. Qian, J. Mu, W. Geng, X. Hou and X. Chou, A stretchable piezoelectric elastic composite, *Mater. Lett.* **236**, 96 (2019).

[14]S. A. Wilson, G. M. Maistros and R. W. Whatmore, Structure modification of 0–3 piezoelectric ceramic/polymer composites through dielectrophoresis, *J. Phys. D: Appl. Phys*. **38**, 175 (2005).

[15]H. Khanbareh, V. Yu. Topolov and C. R. Bowen, *Piezo-Particulate Composites. Manufacturing, Properties, Applications* (Springer Nature Switzerland, Cham, 2019).

[16]H. Khanbareh, K. de Boom, S. van der Zwaag and W.A. Groen, Highly sensitive piezo particulate-polymer foam composites for robotic skin application, *Ferroelectrics* **515**, 25 (2017).

[17]F.-Z. Yao, K. Wang and J.-F. Li, J. Comprehensive investigation of elastic and electrical properties of Li/Ta-modified (K,Na)NbO_3 lead-free piezoceramics, *J. Appl. Phys*. **113**, 174105 (2013).

[18]L. Qiao, G. Li, H. Tao, J. Wu, Z. Xu and F. Li, Full characterization for material constants of a promising KNN-based lead-free piezoelectric ceramic, *Ceram. Int.* **46**, 5641 (2020).

[19]R. E. Newnham, D. P. Skinner and L. E. Cross, Connectivity and piezoelectric — pyroelectric composites, *Mater. Res. Bull*. **13**, 525 (1978).

[20]M. L. Dunn and M. Taya, Micromechanics predictions of the effective electroelastic moduli of piezoelectric composites, *Internat. J. Solids Struct*. **30**, 161 (1993).

[21]J. H. Huang and S. Yu, Electroelastic Eshelby tensors for an ellipsoidal piezoelectric inclusion, *Composites Eng.* **4**, 1169 (1994).

[22]M. L. Dunn and M. Taya, Electromechanical properties of porous piezoelectric ceramics. *J. Am. Ceram. Soc*. **76**, 1697 (1993).

[23]T. Ikeda, *Fundamentals of Piezoelectricity* (Oxford University Press, Oxford, 1990).

[24]J. I. Roscow, H. Pearce, H. Khanbareh, S. Kar-Narayan and C. R. Bowen, Modified energy harvesting figures of merit for stress- and strain-driven piezoelectric systems, *Eur. Phys. J. Special Topics* **228**, 1537 (2019).

[25]K. E. Evans and K. L. Alderson, The static and dynamic moduli of auxetic microporous polyethylene, *J. Mater. Sci. Lett*. **11**, 1721 (1992).

[26]V. Yu. Topolov, P. Bisegna and C. R. Bowen, *Piezo-Active Composites. Microgeometry — Sensitivity Relations* (Springer Internat., Cham, 2018).

[27]V. Yu. Topolov, P. Bisegna and C. R. Bowen, Analysis of the piezoelectric performance of modern 0–3-type composites based on relaxor-ferroelectric single crystals, *Ferroelectrics* **413**, 176 (2011).

[28]M. Fukushima, T. Fujiwara, T. Fey and K. Kakimoto, One- or two-dimensional channel structures and properties of piezoelectric composites via freeze-casting, *J. Am. Ceram. Soc.* **100**, 5400 (2017).

[29]N. K. James, D. B. Deutz, R. K. Bose, S. van der Zwaag and P. Groen, High piezoelectric voltage coefficient in structured lead-free (K, Na, Li)NbO_3 particulate — epoxy composites, *J. Am. Ceram. Soc*. **99**, 3957 (2016).